

Published in final edited form as:

*Biochemistry*. 2012 August 28; 51(34): 6838–6846. doi:10.1021/bi300693k.

## Identification of contact sites between ankyrin and band 3 in the human erythrocyte membrane

Jesse L. Grey<sup>1</sup>, Gayani C. Kodippili<sup>1</sup>, Katya Simon<sup>1</sup>, and Philip S. Low<sup>1,\*</sup>

<sup>1</sup>Department of Chemistry, Purdue University, 560 Oval Dr., West Lafayette, IN 47907, USA

### Abstract

The red cell membrane is stabilized by a spectrin/actin-based cortical cytoskeleton connected to the phospholipid-bilayer via multiple protein bridges. By virtue of its interaction with ankyrin and adducin, the anion transporter, band 3 (AE1), contributes prominently to these bridges. In a previous study, we demonstrated that an exposed loop comprising residues 175–185 of the cytoplasmic domain of band 3 (cdB3) constitutes a critical docking site for ankyrin on band 3. In this paper, we demonstrate that an adjacent loop, comprising residues 63–73 of cdB3, is also essential for ankyrin binding. Data in support of this hypothesis include: 1) deletion or mutation of residues within the latter loop abrogates ankyrin binding without affecting cdB3 structure or its other functions, 2) association of cdB3 with ankyrin is inhibited by competition with the loop peptide, and 3) resealing of the loop peptide into erythrocyte ghosts alters membrane morphology and stability.

To characterize cdB3-ankyrin interaction further, we identified their interfacial contact sites using molecular docking software and the crystal structures of D<sub>3</sub>D<sub>4</sub>-ankyrin and cdB3. The best fit for the interaction reveals multiple salt bridges and hydrophobic contacts between the two proteins. The most important ion pair interactions are: i) cdB3 K69 to ankyrin E645, ii) cdB3 E72 to ankyrin K611, and iii) cdB3 D183 to ankyrin N601 and Q634. Mutation of the above four residues on ankyrin yielded an ankyrin with native CD spectrum, but little or no affinity for cdB3. These data define the docking interface between cdB3 and ankyrin in greater detail.

### INTRODUCTION

The stability of the human erythrocyte membrane depends on the integrity of protein bridges that tether its spectrin/actin-based cortical cytoskeleton to the phospholipid bilayer.<sup>1–78, 9</sup> Although multiple proteins likely contribute to these anchoring interactions,<sup>2, 8–17</sup> data on the molecular bases of hereditary hemolytic anemias together with information on biochemical perturbations that compromise membrane structure suggest that the band 3-ankyrin-spectrin bridge plays a critical role in maintaining membrane stability.<sup>11, 18–21</sup> Thus,

Address correspondence to Philip S. Low (plow@purdue.edu), 7654945273.

Author contributions: P.S.L., J.L.G and G.C.K. designed the research; J.L.G. synthesized the peptide conjugate. J.L.G and G.C.K created mutants; J.L.G and G.C.K performed experiments; K.S discovered the new ankyrin binding loop on cdb3; P.S.L. J.L.G and G.C.K. wrote the paper. The authors declare no conflict of interest

#### Supporting Information

Analysis of the native, reversible, pH-dependent conformational change in cdB3 and the loop 1 deletion mutant (cdB3 ΔL1) the intrinsic fluorescence of both proteins doubles as a function of pH (Figure S1). Inhibition of GAPDH turnover of cdB3 and cdB3 ΔL1 was measured by dialyzing against 10 mM imidazole acetate, 0.1 mM EDTA, 0.5 mM sodium arsenate and 1 mM phosphate at pH 7.0 and incubating with 2 μg/mL GAPDH for 2 min at room temperature (Figure S2). To confirm that mutations introduced into ankyrin (N601D, K611E, Q634E, and E645K) did not perturb the global folding state of the protein, circular dichroism spectra of wild-type and mutant D3D4-ankyrins were compared (Figure S3). Alignment of cdB3 loop 1 (left) and loop 2 (right) sequences among band 3 homologs reported to date using the alignment program MUSCLE (Figure S4). This material is available free of charge via the Internet at <http://pubs.acs.org>.

inherited defects in either band 3 or ankyrin,<sup>22–28</sup> or addition of peptides or proteins that weaken the band 3-ankyrin bridge significantly compromise red cell membrane integrity.<sup>11, 18</sup>

Although the band 3-ankyrin interaction has been studied extensively,<sup>2, 4, 13, 14, 21, 28–37</sup> the specific amino acids involved in stabilizing their association remain elusive. Previous site-directed mutagenesis studies from our lab have revealed a loop comprising residues 175–185 on the cytoplasmic domain of band 3 (cdB3) that serves as a binding site for ankyrin.<sup>38</sup> In fact, deletion of this loop abrogates ankyrin binding *in vitro* without affecting any other band 3-peripheral protein interaction. Surprisingly, however, erythrocytes from transgenic mice expressing only the loop-deleted band 3 exhibit a mild phenotype, suggesting that additional interactions *in vivo* must stabilize the band 3-ankyrin interaction. Recent site-directed spin label data from Beth and colleagues<sup>14</sup> together with biochemical data from other labs<sup>7, 21, 39, 40</sup> have suggested that sequences between residues 70 and 302 on band 3 and between 491 and 722 on ankyrin are also important in stabilizing this association.

To obtain more information on the specific residues responsible for binding of band 3 to ankyrin, we explored the crystal structures of both cdB3<sup>41</sup> and the D3D4 domains of ankyrin<sup>29</sup> to identify likely regions of interfacial contact. From these analyses it became obvious that a second loop, comprising residues 63–73 of band 3, was located directly adjacent to loop 175–185 of band 3 and protruded from band 3 in a manner that would place it in position to make significant contact with ankyrin (Fig. 1). Complementary residues on ankyrin were also implicated. To test these predictions, we mutated several critical residues in both proteins and examined the consequences of these mutations on the affinity of cdB3 for ankyrin. The data below provide much greater detail on the interfacial contacts that stabilize the association of band 3 with ankyrin.

## EXPERIMENTAL PROCEDURES

### Materials

Isopropyl- $\beta$ -D-thiogalactoside (IPTG), phenylmethanesulfonyl fluoride (PMSF), and 1,3-dithiothreitol (DTT) were obtained from RPI Corporation. Imidazole, sodium dibasic phosphate, sodium chloride, and potassium chloride purchased from Sigma Aldrich. Protein concentrations were determined by microBCA assay (Pierce) or by absorbance at 280 nm using calculated extinction coefficients (ExPASy-ProtParam). Purification of recombinant proteins was performed using GST-agarose (Pierce), Ni-NTA agarose (GE-Lifesciences), Co-NTA agarose (BioRad) or Q-Sepharose fast flow beads (GE-Lifesciences). Oligonucleotide-directed mutagenesis was performed using the QuickChange and Lightning QuickChange (multi) mutagenesis kits (Stratagene). Oligonucleotides were synthesized and purified by Integrated DNA Technologies. The synthetic cdB3 (63–74) peptide containing NH<sub>2</sub>- and COOH-terminal cysteines was synthesized by solid phase methodology and purified using reverse-phase C<sub>18</sub> chromatography (Agilent Technologies). Human blood was freshly drawn from patients into acid-citrate dextrose (ACD) treated VacuTainer<sup>TM</sup> tubes (Thermo Scientific). Plasmids were purified using Wizard SV-miniprep kits (Promega), and the cdB3 plasmid encoding a COOH-terminal hexahistidine-tag was donated by Haiyan Chu (Low lab). The GST-D<sub>3</sub>D<sub>4</sub>-ankyrin was a kind gift from Dr. Van Bennett (Duke University).

### Site-specific Mutagenesis

To prepare mutant cdB3s containing a diglycine bridge in place of the loops comprising residues 63–73 and/or 175–185, the following PCR primers were used in combination with the pT7–7 cdB3-His<sub>6</sub> plasmid template<sup>42</sup>: For loop1 deletion mutant 5′-gtctatgtggagctgcagggaggatgggatggaggcggcgcg-3′; For loop 2 deletion mutant 5′-

ggccctgggggtgtgaagggtggacagcctctgtccccaac-3', For the combination of loop 1 and loop 2 deletion mutant, the plasmid containing the loop 1 deletion mutant was mutated with the PCR primer for the loop 2 deletion mutant.

For preparation of the mutated D<sub>3</sub>D<sub>4</sub> domain of ankyrin, the following oligonucleotides were used in simultaneously with combination of the pGEX-KG GST-D<sub>3</sub>D<sub>4</sub> plasmid template with the aid of the Lightning QuickChange (multi) mutagenesis kit (Stratagene):

[N601D]: 5'-acagccctgcctgggatggctacaccctttg-3';

[K611E]: 5'-ttgcacatcgctgccgaacagaaccaggtggag-3';

[Q634E]: 5'-aacgccgagtcggtggaaggtgtgacgccctt-3';

[E645K]: 5'-cacctggccgccagaaaggccacgcagatg-3'.

All cDNAs were amplified and sequenced to confirm the desired mutations. For expression of recombinant proteins, *E. coli* strain BL21 (DE3) pLysS (Invitrogen) was employed.

### Protein Expression and Purification

Wild-type or mutant cdB3 was expressed in the pT7-7 bacterial expression system. Bacteria were induced at an OD<sub>600</sub> of ~0.7 using 0.8 mM IPTG for 3 h at 37°C. The bacteria were lysed with the aid of a French press in Ni-NTA binding buffer (10 mM Imidazole, 30 mM PO<sub>4</sub><sup>3-</sup>, 150 mM NaCl, pH 8.0, and 1 mM PMSF) and eluted from the Ni-NTA agarose beads with the same buffer containing 250 mM imidazole. The proteins were further purified using Q-Sepharose Fast-Flow Anion Exchange chromatography.

GST-ankyrin or the above mutant GST-ankyrin was expressed and purified using glutathione-Sepharose chromatography (GE-Lifesciences). Briefly, BL21 (DE3) pLysS bacteria containing either the wild-type or mutated pGEX-KG ankyrin plasmid were grown to an OD<sub>600</sub> of ~0.5 and induced with 1 mM IPTG for 3 hours. Bacteria were lysed in GST-binding buffer (PBS, pH 7.4) and eluted from glutathione-agarose resin with 20 mM reduced glutathione, 10 mM HPO<sub>4</sub><sup>2-</sup>, pH 8.0, containing a protease cocktail (Protease cocktail V, Pierce).

### Characterization of Expressed Proteins

Expressed cytoplasmic domain of band 3 containing a COOH-terminal His<sub>6</sub>-tag was analyzed by SDS-PAGE and Western blotting with a polyclonal anti-band 3 antibody prepared locally. To confirm that the various loop deletion mutants of cdB3 did not perturb global cdB3 structure, the intrinsic fluorescence of wild-type and mutant cdB3s were determined as a function of pH (the intrinsic fluorescence doubles in wild-type cdB3 due to a major reversible conformation change<sup>43</sup>). Proteins were individually dialyzed into solutions of 50 mM sodium borate, 50 mM sodium phosphate, 70 mM NaCl adjusted to various pH between 6.0 and 11.0, and the intrinsic fluorescence emission at 340 nm was measured using an excitation at 290 nm.

Sedimentation velocity experiments on wild type cdB3 and mutated cdB3 were performed using a Beckman XLI (Beckman-Coulter, Fullerton, CA, USA). Each experiment was conducted at 45,000 rpm for 10 hours at 20°C. The sample and reference chambers were filled with 420 µL of PBS buffer (pH 7.4), containing cdB3 at a concentration of 0.1, 0.2, 0.4 and 0.8 mg/ml. The concentration of cdB3 ΔL1 was 0.8 mg/mL. The density of the buffer, measured on an Anton-Paar DMA 5000 density meter, was 1.00539 g/cm<sup>3</sup>. The partial specific volume (0.7306 mL/g) of wild type and mutant cdB3s and buffer viscosity (0.01043p) were calculated from the protein sequence and buffer composition using SedNterp v.1.09 (<http://www.rasmb.bbri.org/rasmb/windows/sednterp-philos>). The samples

were equilibrated to 20°C for 1 hour prior to centrifugation. Data collection was conducted at 4–5 minute intervals using both Rayleigh interference and absorbance optics at 280 nm. The calculations of the sedimentation coefficient distributions were performed using SEDFIT v. 11.8.<sup>44</sup>

A functional characteristic of cdB3 is its ability to inhibit the catalytic activity of glyceraldehyde-3-phosphate dehydrogenase (GAPDH). To further establish that deletion of loop 63–73 did not measurably perturb other functional properties of cdB3, the mutant protein was assayed for its GAPDH inhibitory potency. For this purpose, desired proteins were dialyzed against 10 mM imidazole acetate, 0.1 mM EDTA, 0.5 mM sodium arsenate and 1 mM phosphate, pH 7.0, and incubated with 2 µg/mL GAPDH for 2 min at room temperature. GAPDH substrates NAD and glyceraldehyde-3-phosphate were added and the absorbance change at 340 nm was measured over the next 180 seconds.

Mutated ankyrin was characterized by SDS-PAGE and Western blot analysis using a polyclonal anti-ankyrin antibody. To confirm that the introduced mutations did not perturb the structure of GST-ankyrin, the CD spectra of the native and mutated ankyrins were examined by circular dichroism using a JASCO (J810) spectropolarimeter. Proteins were dialyzed into 10 mM phosphate buffer, pH 8.0, containing 0.1 M NaF adjusted to a final concentration of 0.5mg/ml, and their molar ellipticities were determined between 200 and 270 nm.

### Analysis of the Affinity of Ankyrin for cdB3

Purified His<sub>6</sub>-tagged normal and mutant cdB3s were incubated overnight with increasing concentrations of GST-ankyrin at 4°C in binding buffer (7.5 mM Na<sub>2</sub>HPO<sub>4</sub>, 90 mM KCl, 10 mM imidazole, 10% sucrose, 1 mg/ml bovine serum albumin, and 1 mM phenylmethanesulfonyl fluoride, pH 8.0). Co<sup>2+</sup>-NTA agarose beads equilibrated in the same buffer were then added and the protein mixtures were agitated for 2 h at 4°C before washing the beads 3x with six volumes of binding buffer. To ensure that equivalent amounts of cdB3 and mutant cdB3s were immobilized on the Co<sup>2+</sup>-beads, captured protein complexes were eluted with 7.5 mM Na<sub>2</sub>HPO<sub>4</sub>, 90 mM KCl, 250 mM imidazole, and 1 mM phenylmethanesulfonyl fluoride, pH 8.0, and compared using an anti-cdB3 antibody. The amount of ankyrin bound to each protein complex was then determined by either dot blot assay using an anti-ankyrin polyclonal antibody or by measuring GST-activity in the supernatant.<sup>45</sup> When desired for competition studies, GST-ankyrin was pre-incubated for 2h with increasing concentrations of a synthetic peptide comprising residues 63–73 of cdB3 prior to addition of cdB3.

### Peptide Resealing into Red Cells

To observe the effect of the synthetic cdB3 peptide on human red blood cell morphology, the peptide was resealed into human red blood cells using the following methodology adapted from<sup>11, 19</sup> with modifications. Briefly, blood collected from healthy volunteers into acid-citrate dextrose was centrifuged, and the buffy-coat and plasma were aspirated. The packed red cells were then washed 3X in two volumes of phosphate-buffered saline (PBS) containing 5 mM glucose and centrifuged at 1000×g. The supernatant was aspirated and 200 µL of packed RBCs were resuspended in PBS containing 5 mM glucose and 2 mM MgCl<sub>2</sub> with various concentrations of synthetic peptide (0 µM (control), 6 µM, 12 µM, or 30 µM). To reseat the peptide into the red blood cells, the mixtures were flash frozen in liquid N<sub>2</sub> for 40s and then equilibrated in a room temperature water bath until thawed. The porous red cells were then resealed by submersion in a 37°C water bath for 45 minutes with gentle shaking. To remove excess peptide, the resealed red cells were washed 4–5 times with PBS containing 5 mM glucose and 0.5% bovine serum albumin. Microscope images were

obtained with a 100x oil immersion lens. Analyses of the same resealed ghosts by ektacytometry was performed as described in literature.<sup>46</sup>

### Simulated Docking of cdB3 and Ankyrin

The crystal structure of the D3D4 domains of ankyrin (1N11) was docked to the crystal structure of cdB3 (1HYN) using WebLabViewer Pro4.0 (2000) with the following constraints: i) no surface charge can be buried during protein binding unless it is paired with an oppositely charged residue on the apposing surface, ii) surface complementarity should be optimized, and iii) hydrogen bonding should be maximized. Possible interfacial sites were further delimited by the following criteria: 1) both loops on cdB3 must make significant contact with D3D4 ankyrin, and 2) the cdB3 binding site on ankyrin must reside near repeats 22 and 23, as previously demonstrated by Michaely et al.,<sup>29</sup> Kim et al.,<sup>14</sup> and Davis et al.<sup>6</sup> While multiple contact regions and orientations of the two proteins were explored, the best fit based on the above criteria yielded the following prominent H-bonding contacts: cdB3 lys-69/ank glu-645, cdB3 glu-72/ank lys-611, and cdB3 asp-183/ank gln-634/asn-601. Therefore, to test the validity of the proposed docking contacts, the above residues on ankyrin were mutated to the oppositely charged amino acids and the effect of these substitutions on cdB3-ankyrin affinity was determined.

## RESULTS

### Characterization of Loop 1 Deleted cdB3

Several lines of evidence support the hypothesis that a second binding site on band 3, in addition to the surface-exposed loop comprising residues 175–185 (hereafter referred to as loop 2)<sup>21</sup>, might exist for ankyrin (see Introduction). Scrutiny of the topography of cdB3 in regions adjacent to loop 2 reveals a similar loop composed of residues 63–73 (hereafter referred to as loop 1) that together with loop 2 forms a pair of “rabbit ears” that extend from the surface of cdB3 in the same direction (Fig. 1).<sup>41</sup> We hypothesized that this newly identified loop 1 might constitute a second docking site for ankyrin. To test this hypothesis, the newly discovered loop 1 was replaced by site-directed mutagenesis with a diglycine bridge that exactly spans the distance at the base of loop 1. This mutant cdB3 (termed  $\Delta$ L1) was then characterized to assure that it retained its native structure and function, after which it was examined for its affinity for the band 3 binding domain (D<sub>3</sub>D<sub>4</sub>) of ankyrin.

Mutated cdB3  $\Delta$ L1 was first shown to exhibit the anticipated molecular weight ( $M_r \sim 43$ kDa) by SDS-PAGE and Western blotting using a polyclonal antibody against cdB3 (data not shown). Next, because native cdB3 is known to exist as a tight dimer in physiological buffers<sup>1, 41, 47</sup>, mutated cdB3  $\Delta$ L1 was also examined for its quaternary structure. Importantly, sedimentation velocity analysis of cdB3  $\Delta$ L1 on a Beckman XLI ultracentrifuge revealed only a dimeric cdB3  $\Delta$ L1, with no evidence of either monomer or tetramer cdB3 (data not shown). Thirdly, to evaluate whether deletion of residues 63–73 (loop 1) might perturb the native conformation of cdB3  $\Delta$ L1, the pH dependence of its intrinsic fluorescence was measured between pH 6 and 11. As seen in supplementary Fig. 1, the unusual doubling of intrinsic fluorescence that is known to characterize a native conformational change in wild type cdB3<sup>1, 47</sup> remains present in cdB3  $\Delta$ L1, suggesting that the global structure and conformational flexibility of the mutated protein is essentially native. Finally, to assure that a diagnostic function of native cdB3, namely its ability to inhibit the catalytic activity of GAPDH, has also remained unaltered, the abilities of wild type and cdB3  $\Delta$ L1 to suppress GAPDH activity were compared. As shown in supplemental Fig. 2, both proteins were found to inhibit GAPDH to essentially the same degree; i.e. 90% inhibition for the wild-type protein and 85% for the loop deletion mutant.



## Analysis of Mutant cdB3 Affinity for Ankyrin Using Pull-down Assays

To obtain an initial indication of the affinity of cdB3  $\Delta$ L1 for ankyrin, binding of D<sub>3</sub>D<sub>4</sub> ankyrin to both cdB3  $\Delta$ L1 and native cdB3 was evaluated by a His-tag pull-down assay. For this purpose, His-tagged native cdB3 or His-tagged mutant cdB3 was incubated with increasing concentrations of GST-D<sub>3</sub>D<sub>4</sub>-ankyrin and any complexes formed were captured onto Co<sup>2+</sup>-NTA agarose beads. The amount of captured ankyrin was then determined by dot-blot analysis or evaluation of GST activity retained on the beads. As seen in Fig. 2A, when the eluted complexes were blotted onto nitrocellulose and probed with anti-ankyrin polyclonal antibodies, little or no evidence for GST-ankyrin binding to cdB3  $\Delta$ L1 was found, even though the usual prominent binding of ankyrin to native His-tagged cdB3 was observed. These data suggest that cdB3  $\Delta$ L1 may exhibit weak or no affinity for ankyrin.

To more quantitatively assess the affinities of native and cdB3  $\Delta$ L1 for ankyrin, the aforementioned beads containing GST-D<sub>3</sub>D<sub>4</sub>-ankyrin/cdB3 complexes were also assayed for GST activity. As shown in Fig. 2B, no difference in affinity between heat-denatured cdB3 and cdB3  $\Delta$ L1 could be detected. Moreover, in agreement with previously published results,<sup>38</sup> binding of native cdB3 to D<sub>3</sub>D<sub>4</sub> ankyrin was characterized by an apparent dissociation constant of ~400 nM. While this K<sub>d</sub> is clearly weaker than the dissociation constant of band 3 for intact ankyrin,<sup>7</sup> it should be remembered that regions of ankyrin external to the D<sub>3</sub>D<sub>4</sub> domain are also known to participate in band 3 binding.<sup>7</sup> As additional controls, strong affinity for GST-ankyrin was demonstrated using immobilized cdB3  $\Delta$ 1–50 (a deletion mutant known to retain its native ankyrin affinity),<sup>41</sup> whereas no affinity could be detected for immobilized  $\Delta$ L2 cdB3,<sup>21</sup> double loop deleted ( $\Delta$ L1 +  $\Delta$ L2) cdB3, heat denatured cdB3, or kidney cdB3 (a spliceoform of cdB3 expressed in the kidney that is known to display no affinity for ankyrin).<sup>48</sup> These data suggest that loop 1 comprising residues 63–73 of cdB3 are essential for ankyrin binding.

To further confirm the importance of loop 1 in promoting the ankyrin-band 3 interaction, the converse of the above experiments was also performed. In this case, GST-ankyrin (1  $\mu$ M) was first immobilized onto glutathione-beads, after which the beads were incubated with either cdB3 (1  $\mu$ M) or cdB3  $\Delta$ L1 (1  $\mu$ M). As demonstrated in the dot-blot analysis of the captured complexes (Fig. 2C), loop deletion cdB3 again displayed no affinity for ankyrin, whereas native cdB3 exhibited strong affinity. These data confirm the hypothesis that loop 1 is critical for ankyrin association.

## Competition of Loop 1 Peptide for Ankyrin Binding to cdB3

To further document the importance of cdB3 loop 1 to ankyrin binding, a synthetic peptide designed to mimic the exposed loop on cdB3 was synthesized. For this purpose, a peptide comprising residues 63–73 of cdB3 was linked via a normal peptide bond at its NH<sub>2</sub>- and COOH-termini to a cysteine residue, which in turn was oxidized to form a loop containing the intact peptide tethered via a disulfide bond at its ends. To test whether this isolated peptide loop might competitively displace GST-ankyrin from native cdB3, increasing concentrations of the peptide were added to an incubation mixture containing ankyrin and native His-tagged cdB3 (1  $\mu$ M), after which the complexes were captured onto Co<sup>2+</sup>-NTA agarose beads. As seen in Fig. 3, the cyclized peptide competed well for ankyrin-cdB3 binding with an IC<sub>50</sub> of ~15  $\mu$ M, whereas the less entropically favored linear peptide exhibited an IC<sub>50</sub> of only 55  $\mu$ M. While neither of these peptides competed with the affinity of intact ankyrin, their lower affinity was expected since neither peptide can form all of the contacts that exist at the interface of ankyrin with intact band 3.

Finally, to explore whether the cyclized peptide might also compete *in situ* for the band 3-ankyrin interaction, the cyclized peptide was resealed into human erythrocyte ghosts and the

morphologies and stabilities of the resealed ghosts were examined as a function of peptide concentration. While it could not be established that the disulfide bond maintaining the peptide in its cyclized configuration remained intact in the resealed cells, rupture of the ankyrin bridge *in situ* nevertheless proceeded as anticipated, triggering membrane blebbing and a gradual decrease in membrane surface area (Fig. 4A), as seen with previous competitors of the band 3-ankyrin interaction.<sup>11,18</sup> Importantly, this extensive vesiculation at higher peptide concentrations often rendered it difficult to locate large clusters of cells for microscopic observation, probably because many of the cells were simply lost to vesiculation. Moreover, analyses of the same resealed ghosts by ektacytometry<sup>46</sup> demonstrated that the entrapped peptide compromised membrane deformability (Fig. 4B). Together with the above binding studies, these data establish that loop 1 comprising residues 63–73 of band 3 contributes measurably to the stability of the band 3-ankyrin interaction.

### Analysis of the Docking Site of cdB3 with Ankyrin

With documentation of the involvement of two proximal surface loops of cdB3 in ankyrin binding, the question naturally arose whether a complementary docking site on ankyrin might now be identified. Davis and Bennett<sup>4</sup> had previously established that the major binding site for cdB3 on ankyrin resides near the C-terminus of the 89 kDa membrane binding domain, probably between residues 403 and 779 of ankyrin. Although Michaely et al.<sup>7</sup> further observed that deletion of ankyrin repeats 23 and 24 yielded a misfolded protein with no affinity for KI-IOVs, no further definition of band 3's docking site on ankyrin was reported by this initial analysis. However, while preparing our studies for publication, a paper by Beth and coworkers<sup>14</sup> appeared suggesting that much of the contact between band 3 and ankyrin likely resides between ankyrin repeats 18–22. As will be seen below, we have come to a similar conclusion using independent methodologies.

For our analyses, a program termed WebLab ViewerPro was used to optimally dock the crystal structure of cdB3<sup>41</sup> onto the crystal structure of the D<sub>3</sub>D<sub>4</sub> domain of ankyrin.<sup>29</sup> The region of greatest surface charge and topographical complementarity to emerge from this analysis was found to involve multiple hydrophobic and hydrophilic interactions between the two proteins (Fig. 5). Moreover, rather than being restricted to the cdB3 loops examined in this study, several conspicuous interactions were also observed to reside outside these two exposed loops. However, because of our interest in testing whether the identified surface loops were critical to ankyrin binding, we decided to restrict our mutagenesis studies to ankyrin residues predicted to dock with amino acid side chains in the two protruding loops. The most prominent salt bridges to fit this requirement were K69 of cdB3 to E645 of ankyrin, E72 of cdB3 to K611 of ankyrin, and D183 of cdB3 to both Q634 and N601 of ankyrin (Fig. 5). Consequently, the four amino acids implicated on the ankyrin contact surface were mutated to residues projected to disrupt any salt bridge in which they might participate (N601D, K611E, E645K, and Q634E). Analysis of the binding of this mutated ankyrin to cdB3s (Fig. 6) demonstrated that the above conservative mutations renders the D<sub>3</sub>D<sub>4</sub> domains of ankyrin unable to bind cdB3. Given that the same mutations do not induce any conformational perturbations in ankyrin, as documented by the absence of a detectable change in the CD spectrum (supplemental Fig. 3), the data suggest that the predicted salt bridges are important to ankyrin's association with band 3. Nevertheless, because a crystal structure-based analysis of this sort ignores possible conformational changes induced by protein docking, it is not unlikely that additional or even different salt bridges might arise during binding of ankyrin to cdB3 in solution.

## DISCUSSION

Although it was previously demonstrated that a loop comprising residues 175–185 of cdB3 forms at least part of the ankyrin binding site on band 3,<sup>38</sup> several of our own observations

suggested that a second more amino-terminal site might also contribute to ankyrin association: 1) blocking of the NH<sub>2</sub>-terminus of cdb3 by the F<sub>ab</sub> of a monoclonal antibody to residues 1–15 of band 3 inhibits ankyrin binding<sup>33</sup>; 2) association of ankyrin with cdb3 is blocked by phosphorylation of tyrosines 8 and 21 of band 3<sup>49</sup>; 3) phosphorylation of tyrosines 8 and 21 of cdb3 is prevented by ankyrin binding<sup>18</sup>; 4) ankyrin and protein 4.1 are known to compete for binding to the NH<sub>2</sub>-terminus of cdb3,<sup>50</sup> and 5) the biological impact of deletion of loop 2 (i.e. residues 175–185) on erythrocyte stability is surprisingly mild in transgenic mice.<sup>20</sup> Motivated by this information, we analyzed the three-dimensional structure of cdb3 and found another surface-exposed loop (residues 63–73), directly adjacent to the first, that is ideally positioned to participate significantly in ankyrin binding. Studies aimed at evaluating this more NH<sub>2</sub>-terminal loop demonstrate that replacement of the loop with a diglycine bridge that exactly spans the gap created by the deletion mutagenesis eliminates ankyrin binding without altering either cdb3 conformation or any other prominent functional property of the polypeptide. Moreover, mutation of residues within the band 3 binding domain of ankyrin predicted *in silico* to dock with the loops on band 3 was also found to abrogate binding.

Although surface-exposed loops are generally the least conserved sequences in a protein, one might expect the opposite to be true with the two loops that mediate the band 3-ankyrin interaction. As seen in supplemental Fig. 4, this prediction is confirmed among mammalian species, but not verified when the analysis is extended to avian and fish species. Thus, MULTIPLE Sequence Comparison by Log-Expectation (MUSCLE) alignment reveals >75% sequence identity among the nine mammalian sequences available. In contrast, when avian (chicken and finch) band 3 are included in the comparison, only loop 2 displays measurable homology, while when fish (skate, trout and zebrafish) band 3 are added, the homology is limited to loop 1. These data may suggest that the ankyrin-band 3 interaction has been shaped by different evolutionary pressures in different species and that the resulting properties of the final interaction have been tuned to the specific needs of each species.

During preparation of this manuscript, an article from Beth and coworkers<sup>14</sup> appeared that identified a similar band 3-ankyrin interface using very different methodologies. Thus, Beth and colleagues attached spin labels to multiple residues on band 3 and ankyrin, and used DEER (double electron-electron resonance) measurements to estimate distances between the site-specific spin labels. They concluded that a large fraction of the cdb3 surface likely interacts with ankyrin, primarily via hydrophobic interactions. One of the residues that they spin-labeled on cdb3 was Glu72, which fortuitously resides in loop 1 (Fig. 1). Importantly, derivatization of this amino acid was found to inhibit ankyrin binding; i.e. consistent with our conclusion that this loop makes intimate contact with ankyrin. The Beth lab further showed that spin labeling of ankyrin at residues 596 or 598 (ankyrin repeat 18), or residues 629 or 631 (ankyrin repeat 19), or 652 or 664 (ankyrin repeat 20) also partially inhibited cdb3 binding. Since the residues that we mutated on ankyrin to block cdb3 binding (i.e. residues 601, 611, 634, and 645) also reside in ankyrin repeats 19 and 20, strong agreement again is seen between our two methodologies. Although our mutagenesis results only demonstrate that the residues on ankyrin closest to the loops on cdb3 participate in cdb3 binding, further analysis of the simulated docking interface implicates residues outside the exposed cdb3 loops in ankyrin binding. Included among the predicted additional contact sites are Asp 122, Thr 126, Glu 151, Arg 155, and Lys 160 of cdb3. In this comparison with data from other labs, it is interesting to note that Beth and coworkers find that an EPR label attached to Arg 155 of cdb3 inhibits ankyrin binding by ~50%. Moreover, Davis and coworkers demonstrate that antibodies to residues 118–162 of cdb3 also inhibit ankyrin binding (Davis, 1989). While additional contacts undoubtedly contribute to the band 3-ankyrin interaction, the strong congruence seen among multiple labs using different techniques now adds weight to the argument that the ankyrin-band 3 complex is at least



partially stabilized by interactions between the dual loop region on band 3 and repeats 18–20 of ankyrin, as demonstrated above.

Finally, a lesson can be learned from the absence of any colossal effect on erythrocyte stability arising from the engineered deletion of cdB3 loop 2 in transgenic mice. Thus, deletion of loop 2 was found to totally abrogate ankyrin binding when the binding assay was conducted with only the two purified proteins. However, when transgenic mice containing the loop 2 deletion were examined, only mild osmotic fragility, moderate morphological abnormalities, and an elevated reticulocyte count were observed. Because a more severe phenotype was expected, the affinity of ankyrin for loop 2 deleted band 3 was re-examined using KI-IOVs from the transgenic  $\Delta$ L2 mice. As previously observed, no detectable binding was seen. Thus, when peripheral membrane proteins are removed from band 3, deletion of loop 2 alone indeed eliminates ankyrin binding, even though the interaction remains intact in the native erythrocyte. In the present study, ankyrin affinity could similarly be eliminated by deletion of loop 1 on cdB3 (residues 63–73), even with the previously identified loop 2 (residues 175–185) still present. While these results may seem confusing, we believe they teach an important principle; namely, that critical protein-protein interactions are commonly stabilized by multiple interfacial contacts, and that whereas mutation of some of these contacts may shift the binding equilibrium between purified proteins towards total dissociation, in the context of a large multicomponent membrane complex, auxiliary interactions can significantly compensate for defects in the primary interaction. In the context of the band 3-ankyrin bridge to the cytoskeleton, we envision these auxiliary interactions to arise from the simultaneous association of band 3 and ankyrin with protein 4.2,<sup>35, 51</sup> CD47,<sup>8, 52</sup> RhAG,<sup>8</sup> and several glycolytic enzymes. It will be now be interesting to determine whether transgenic mice lacking both loops 1 and 2 will produce erythrocytes that display more pronounced instability *in vivo*.

## Supplementary Material

Refer to Web version on PubMed Central for supplementary material.

## Acknowledgments

P.S.L. acknowledges funding from the National Institute of Health (GM24417-32)

## Abbreviations

<b>cdB3</b>	cytoplasmic domain of band 3
<b>AE1</b>	anion transporter, band 3
<b>CD spectrum</b>	Circular dichroism spectrum
<b>IPTG</b>	Isopropyl- $\beta$ -D-thiogalactoside
<b>PMSF</b>	Phenylmethanesulfonyl fluoride
<b>DTT</b>	1,3-dithiothreitol

## References

1. Low PS, Westfall MA, Allen DP, Appell KC. Characterization of the reversible conformational equilibrium of the cytoplasmic domain of erythrocyte-membrane band-3. J Biol Chem. 1984; 259(21):3070–3076. [PubMed: 6421816]

2. Low PS. Structure and Function of the Cytoplasmic Domain of Band-3 - Center of Erythrocyte-Membrane Peripheral Protein Interactions. *Biochimica Et Biophysica Acta*. 1986; 864(2):145–167. [PubMed: 2943319]
3. Low PS, Allen DP, Zioncheck TF, Chari P, Willardson BM, Geahlen RL, Harrison ML. Tyrosine Phosphorylation of Band-3 Inhibits Peripheral Protein-Binding. *J Biol Chem*. 1987; 262(10):4592–4596. [PubMed: 3558357]
4. Davis L, Lux SE, Bennett V. Mapping the Ankyrin-Binding Site of the Human-Erythrocyte Anion-Exchanger. *J Biol Chem*. 1989; 264(16):9665–9672. [PubMed: 2470759]
5. Thevenin BJM, Low PS. Kinetics and Regulation of the Ankyrin-Band-3 Interaction of the Human Red-Blood-Cell Membrane. *J Biol Chem*. 1990; 265(27):16166–16172. [PubMed: 2144526]
6. Davis LH, Otto E, Bennett V. Specific 33-Residue Repeat(S) of Erythrocyte Ankyrin Associate with the Anion-Exchanger. *J Biol Chem*. 1991; 266(17):11163–11169. [PubMed: 1828247]
7. Michaely P, Bennett V. The Ank Repeats of Erythrocyte Ankyrin Form 2 Distinct but Cooperative Binding-Sites for the Erythrocyte Anion-Exchanger. *J Biol Chem*. 1995; 270(37):22050–22057. [PubMed: 7665627]
8. Bruce LJ, Ghosh S, King MJ, Layton DM, Mawby WJ, Stewart GW, Oldenburg PA, Delaunay J, Tanner MJA. Absence of CD47 in protein 4.2-deficient hereditary spherocytosis in man: an interaction between the Rh complex and the band 3 complex. *Blood*. 2002; 100(5):1878–1885. [PubMed: 12176912]
9. Bruce LJ, Beckmann R, Ribeiro ML, Peters LL, Chasis JA, Delaunay J, Mohandas N, Anstee DJ, Tanner MJA. A band 3-based macrocomplex of integral and peripheral proteins in the RBC membrane. *Blood*. 2003; 101(10):4180–4188. [PubMed: 12531814]
10. Bennett V, Gilligan DM. The spectrin-based membrane skeleton and micron-scale organization of the plasma membrane. *Annu Rev Cell Biol*. 1993; 9:27–66. [PubMed: 8280463]
11. Anong WA, Franco T, Chu HY, Weis TL, Devlin EE, Bodine DM, An XL, Mohandas N, Low PS. Adducin forms a bridge between the erythrocyte membrane and its cytoskeleton and regulates membrane cohesion. *Blood*. 2009; 114(9):1904–1912. [PubMed: 19567882]
12. Mohandas N, Chasis JA. Red-Blood-Cell Deformability, Membrane Material Properties and Shape - Regulation by Transmembrane, Skeletal and Cytosolic Proteins and Lipids. *Semin Hematol*. 1993; 30(3):171–192. [PubMed: 8211222]
13. Khan AA, Hanada T, Mohseni M, Jeong JJ, Zeng LX, Gaetani M, Li DH, Reed BC, Speicher DW, Chishti AH. Dematin and adducin provide a novel link between the spectrin cytoskeleton and human erythrocyte membrane by directly interacting with glucose transporter-1. *J Biol Chem*. 2008; 283(21):14600–14609. [PubMed: 18347014]
14. Kim S, Brandon S, Zhou Z, Cobb CE, Edwards SJ, Moth CW, Parry CS, Smith JA, Lybrand TP, Hustedt EJ, Beth AH. Determination of Structural Models of the Complex between the Cytoplasmic Domain of Erythrocyte Band 3 and Ankyrin-R Repeats 13–24. *J Biol Chem*. 2011; 286(23):20746–20757. [PubMed: 21493712]
15. Van Den Akker E, Satchwell TJ, Williamson RC, Toye AM. Band 3 multiprotein complexes in the red cell membrane; of mice and men. *Blood Cell Mol Dis*. 2010; 45(1):1–8.
16. Satchwell TJ, Shoemark DK, Sessions RB, Toye AM. Protein 4.2: A complex linker. *Blood Cell Mol Dis*. 2009; 42(3):201–210.
17. Salomao M, Zhang XH, Yang Y, Lee S, Hartwig JH, Chasis JA, Mohandas N, An XL. Protein 4.1R-dependent multiprotein complex: New insights into the structural organization of the red blood cell membrane. *Proc Nat Acad Sci USA*. 2008; 105(23):8026–8031. [PubMed: 18524950]
18. Bruce LJ, Ring SM, Ridgwell K, Reardon DM, Seymour CA, Van Dort HM, Low PS, Tanner MJA. Southeast Asian ovalocytic (SAO) erythrocytes have a cold sensitive cation leak: implications for in vitro studies on stored SAO red cells. *Biochim Biophys Acta*. 1999; 1416(1–2): 258–270. [PubMed: 9889381]
19. Van Dort HM, Knowles DW, Chasis JA, Lee G, Mohandas N, Low PS. Analysis of integral membrane protein contributions to the deformability and stability of the human erythrocyte membrane. *J Biol Chem*. 2001; 276(50):46968–46974. [PubMed: 11595743]
20. Stefanovic M, Markham NO, Parry EM, Garrett-Beal LJ, Cline AP, Gallagher PG, Low PS, Bodine DM. An 11-amino acid beta-hairpin loop in the cytoplasmic domain of band 3 is

- responsible for ankyrin binding in mouse erythrocytes. *Proc Nat Acad Sci USA*. 2007; 104(35): 13972–13977. [PubMed: 17715300]
21. Chang SH, Low PS. Identification of a critical ankyrin-binding loop on the cytoplasmic domain of erythrocyte membrane band 3 by crystal structure analysis and site-directed mutagenesis. *J Biol Chem*. 2003; 278(9):6879–6884. [PubMed: 12482869]
  22. Coetzer TL, Lawler J, Liu SC, Prchal JT, Gualtieri RJ, Brain MC, Dacie JV, Palek J. Partial ankyrin and spectrin deficiency in severe, atypical hereditary spherocytosis. *N Engl J Med*. 1988; 318(4):230–234. [PubMed: 2961992]
  23. Costa FF, Agre P, Watkins PC, Winkelmann JC, Tang TK, John KM, Lux SE, Forget BG. Linkage of Dominant Hereditary Spherocytosis to the Gene for the Erythrocyte Membrane-Skeleton Protein Ankyrin. *N Engl J Med*. 1990; 323(15):1046–1050. [PubMed: 1977081]
  24. Lux SE, Tse WT, Menninger JC, John KM, Harris P, Shalev O, Chilcote RR, Marchesi SL, Watkins PC, Bennett V, et al. Hereditary spherocytosis associated with deletion of human erythrocyte ankyrin gene on chromosome 8. *Nature*. 1990; 345(6277):736–739. [PubMed: 2141669]
  25. Hanspal M, Yoon SH, Yu H, Hanspal JS, Lambert S, Palek J, Prchal JT. Molecular-Basis of Spectrin and Ankyrin Deficiencies in Severe Hereditary Spherocytosis - Evidence Implicating a Primary Defect of Ankyrin. *Blood*. 1991; 77(1):165–173. [PubMed: 1702027]
  26. De Falco, L.; De Franceschi, L.; Borgese, F.; Piscopo, C.; Esposito, M.; Avvisati, R.; Izzo, P.; Guizouarn, H.; Biondani, A.; Iolascon, A. BAND 3CEINGE (Gly796Arg) Mutation Causes Dehydrated Hereditary Stomatocytosis (DHS) with Dyserythropoietic Phenotype. 50th Annual Meeting of the American-Society-of-Hematology, Blood; San Francisco, CA. 2008. p. 2874
  27. Savvides P, Shalev O, John KM, Lux SE. Combined Spectrin and Ankyrin Deficiency Is Common in Autosomal-Dominant Hereditary Spherocytosis. *Blood*. 1993; 82(10):2953–2960. [PubMed: 8219186]
  28. Hassoun H, Vassiliadis JN, Murray J, Njolstad PR, Rogus JJ, Ballas SK, Schaffer F, Jarolim P, Brabec V, Palek J. Characterization of the underlying molecular defect in hereditary spherocytosis associated with spectrin deficiency. *Blood*. 1997; 90(1):398–406. [PubMed: 9207476]
  29. Michaely P, Tomchick DR, Machius M, Anderson RGW. Crystal structure of a 12 ANK repeat stack from human ankyrinR. *Embo Journal*. 2002; 21(23):6387–6396. [PubMed: 12456646]
  30. Bennett V, Stenbuck PJ. Association between Ankyrin and the Cytoplasmic Domain of Band-3 Isolated from the Human-Erythrocyte Membrane. *J Biol Chem*. 1980; 255(13):6424–6432. [PubMed: 6446557]
  31. Burton NM, Bruce LJ. Modelling the structure of the red cell membrane. *Biochem cell biol*. 2011; 89(2):200–215. [PubMed: 21455271]
  32. Hughes MR, Anderson N, Maltby S, Wong J, Berberovic Z, Birkenmeier CS, Haddon DJ, Garcha K, Flenniken A, Osborne LR, Adamson SL, Rossant J, Peters LL, Minden MD, Paulson RF, Wang C, Barber DL, McNagny KM, Stanford WL. A novel ENU-generated truncation mutation lacking the spectrin-binding and C-terminal regulatory domains of Ank1 models severe hemolytic hereditary spherocytosis. *Exp Hematol*. 2011; 39(3):305–320. [PubMed: 21193012]
  33. Low PS, Willardson BM, Mohandas N, Rossi M, Shohet S. Contribution of the Band 3-Ankyrin Interaction to Erythrocyte-Membrane Mechanical Stability. *Blood*. 1991; 77(7):1581–1586. [PubMed: 1826225]
  34. Rank G, Sutton R, Marshall V, Lundie RJ, Caddy J, Romeo T, Fernandez K, McCormack MP, Cooke BM, Foote SJ, Crabb BS, Curtis DJ, Hilton DJ, Kile BT, Jane SM. Novel roles for erythroid Ankyrin-1 revealed through an ENU-induced null mouse mutant. *Blood*. 2009; 113(14): 3352–3362. [PubMed: 19179303]
  35. Su Y, Ding Y, Jiang M, Jiang WH, Hu XJ, Zhang ZH. Associations of protein 4.2 with band 3 and ankyrin. *Mol Cell Biochem*. 2006; 289(1–2):159–166. [PubMed: 16718373]
  36. Kodippili GC, Spector J, Hale J, Giger K, Hughes MR, McNagny KM, Birkenmeier C, Peters L, Ritchie K, Low PS. Analysis of the mobilities of band 3 populations associated with the ankyrin and junctional complexes in intact murine erythrocytes. *J Biol Chem*. 2012; 286(6):4129–4138. [PubMed: 22147703]

37. Yasunaga M, Ipsaro JJ, Mondragon A. Structurally similar but functionally diverse ZU5 domains in human erythrocyte ankyrin. *J Mol Biol.* 2012 Apr 6; 417(4):336–50. Epub 2012 Jan 30. [PubMed: 22310050]
38. Chang SH, Low PS. Identification of a critical ankyrin-binding loop on the cytoplasmic domain of erythrocyte membrane band 3 by crystal structure analysis and site-directed mutagenesis. *J Biol Chem.* 2003; 278(9):6879–6884. [PubMed: 12482869]
39. Kim S, Brandon S, Zhou Z, Cobb CE, Edwards SJ, Moth CW, Parry CS, Smith JA, Lybrand TP, Hustedt EJ, Beth AH. Determination of Structural Models of the Complex between the Cytoplasmic Domain of Erythrocyte Band 3 and Ankyrin-R Repeats 13–24. *J Biol Chem.* 286(23): 20746–20757. [PubMed: 21493712]
40. Zhou Z, DeSensi SC, Stein RA, Brandon S, Dixit M, McArdle EJ, Warren EM, Kroh HK, Song LK, Cobb CE, Hustedt EJ, Beth AH. Solution structure of the 3 cytoplasmic domain of erythrocyte membrane band 3 determined by site-directed spin labeling. *Biochemistry.* 2005; 44(46):15115–15128. [PubMed: 16285715]
41. Zhang D, Kiyatkin A, Bolin JT, Low PS. Crystallographic structure and functional interpretation of the cytoplasmic domain of erythrocyte membrane band 3. *Blood.* 2000; 96(9):2925–2933. [PubMed: 11049968]
42. Wang CC, Badylak JA, Lux SE, Moriyama R, Dixon JE, Low PS. Expression, Purification, and Characterization of the Functional Dimeric Cytoplasmic Domain of Human Erythrocyte Band-3 in *Escherichia-Coli*. *Protein Sci.* 1992; 1(9):1206–1214. [PubMed: 1304397]
43. Low PS, Zhou JZ, Stefanovic M, Chang SH. Structural and functional characterization of the cytoplasmic domain of band 3 by in vitro mutagenesis. *Blood.* 2001; 98(11):436A–436A. [PubMed: 11435314]
44. Schuck P, Perugini MA, Gonzales NR, Howlett GJ, Schubert D. Size-distribution analysis of proteins by analytical ultracentrifugation: Strategies and application to model systems. *Biophys J.* 2002; 82(2):1096–1111. [PubMed: 11806949]
45. Habig WH, Pabst MJ, Jakoby WB. Glutathione S-Transferases - First Enzymatic Step in Mercapturic Acid Formation. *J Biol Chem.* 1974; 249(22):7130–7139. [PubMed: 4436300]
46. Chasis JA, Mohandas N. Erythrocyte-Membrane Deformability and Stability - 2 Distinct Membrane-Properties That Are Independently Regulated by Skeletal Protein Associations. *J Cell Biol.* 1986; 103(2):343–350. [PubMed: 3733870]
47. Sarna MK, Ingley E, Busfield SJ, Cull VS, Lepere W, McCarthy DJ, Wright MJ, Palmer GA, Chappell D, Sayer MS, Alexander WS, Hilton DJ, Starr R, Watowich SS, Bittorf T, Klinken SP, Tilbrook PA. Differential regulation of SOCS genes in normal and transformed erythroid cells. *Oncogene.* 2003; 22(21):3221–3230. [PubMed: 12761492]
48. Wang CC, Moriyama R, Lombardo CR, Low PS. Partial Characterization of the Cytoplasmic Domain of Human Kidney Band-3. *J Biol Chem.* 1995; 270(30):17892–17897. [PubMed: 7629093]
49. Ferru E, Giger K, Pantaleo A, Campanella E, Grey J, Ritchie K, Vono R, Turrini F, Low PS. Regulation of membrane-cytoskeletal interactions by tyrosine phosphorylation of erythrocyte band 3. *Blood.* 2011; 117(22):5998–6006. [PubMed: 21474668]
50. Workman RF, Low PS. Biochemical analysis of potential sites for protein 4.1-mediated anchoring of the spectrin-actin skeleton to the erythrocyte membrane. *J Biol Chem.* 1998; 273(11):6171–6176. [PubMed: 9497338]
51. Kumpornsin K, Jiemsup S, Yongkiettrakul S, Chookajorn T. Characterization of band 3-ankyrin-Protein 4.2 complex by biochemical and mass spectrometry approaches. *Biochem Biophys Res Commu.* 2011; 406(3):332–335.
52. Van Den Akker E, Satchwell TJ, Pellegrin S, Flatt JF, Maigre M, Daniels G, Delaunay J, Bruce LJ, Toye AM. Investigating the key membrane protein changes during in vitro erythropoiesis of protein 4.2 (–) cells (mutations Chartres 1 and 2). *Haematol Hematol J.* 2010; 95(8):1278–1286.

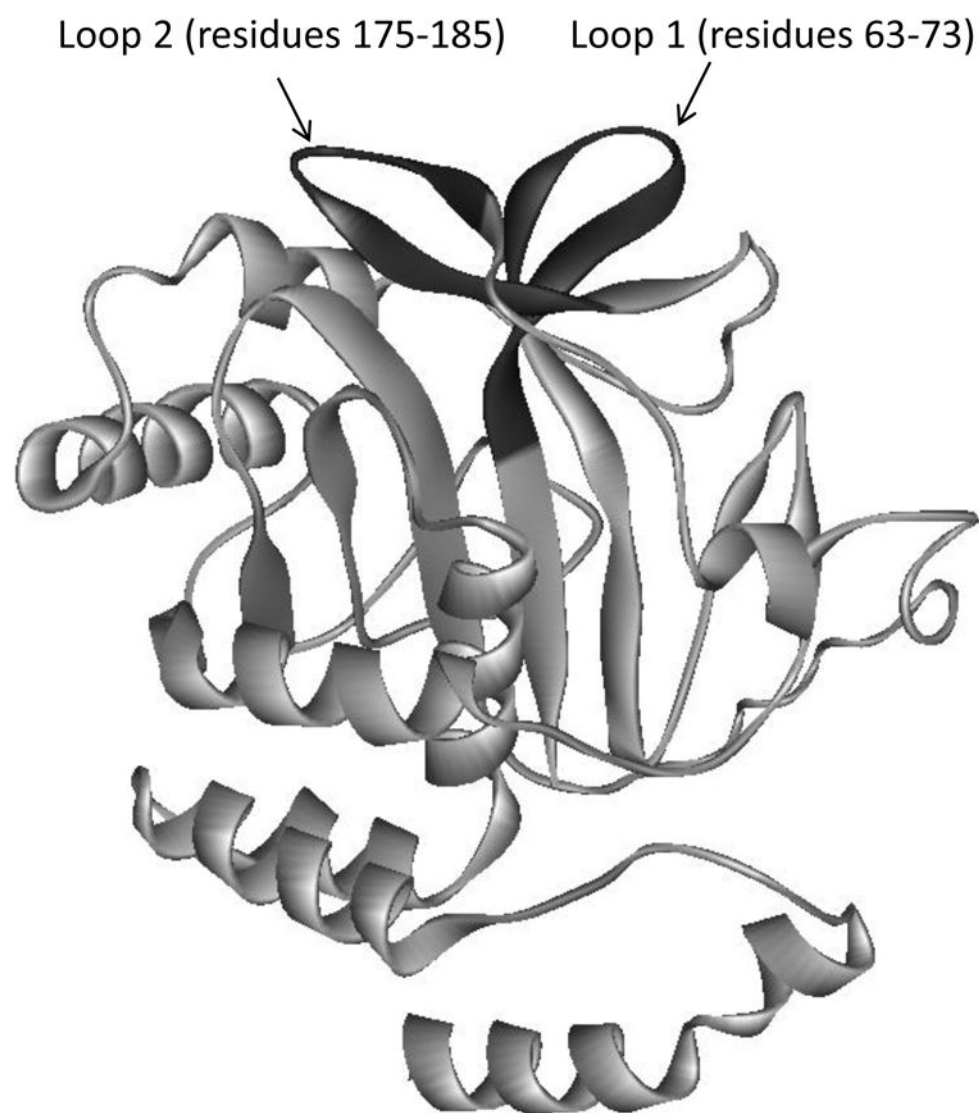


**Figure 1.** Monomeric structure of cdb3<sup>41</sup> showing proposed ankyrin binding loops that protrude from the protein's surface (highlighted in black). The loop comprising residues 175–185 was shown previously to be essential for ankyrin binding.<sup>38</sup> Involvement of the loop comprising residues 63–73 is investigated in this paper



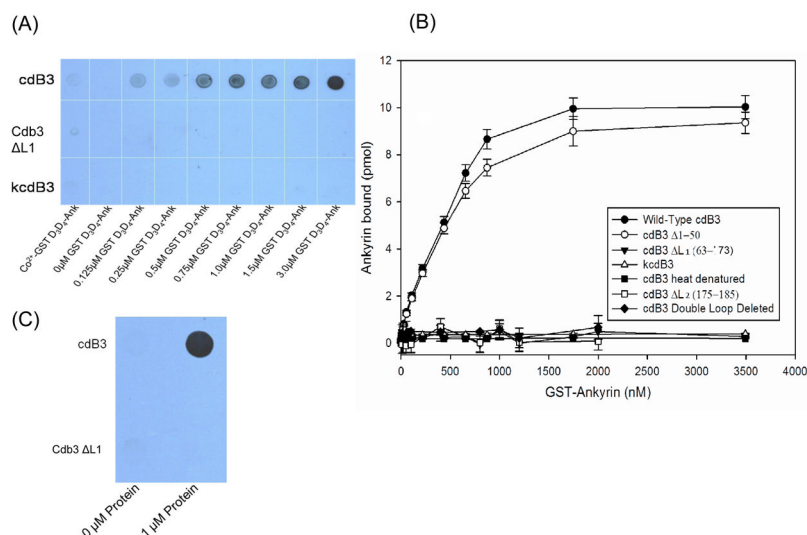


**Figure 2.**

Analysis of the binding of the D<sub>3</sub>D<sub>4</sub> domain of ankyrin to cdb3. His-tagged cdb3 was incubated for 2h with increasing concentrations of a GST fusion construct of the D<sub>3</sub>D<sub>4</sub> domain of ankyrin and then captured onto Co<sup>2+</sup>-NTA agarose beads. After washing 3x with binding buffer, bound protein was eluted and quantitated (A) by immunoblot analysis using an antibody to D<sub>3</sub>D<sub>4</sub> ankyrin, or (B) by measuring GST activity in the eluent (see Methods). (C) Alternatively, GST- D<sub>3</sub>D<sub>4</sub> was incubated for 2 hrs with either wild type or a mutant cdb3 lacking loop 2, and the complexes were captured on GST-Sepharose beads, washed 3x with binding buffer and evaluated for cdb3 content by dot blot analysis using an anti-cdb3 antibody. kcdB3 - kidney cdb3; cdb3 ΔL1 - cdb3 lacking loop 1; cdb3 Δ1-50 - cdb3 lacking loop residues 1-50. Error bars correspond to S.D., where n=2.

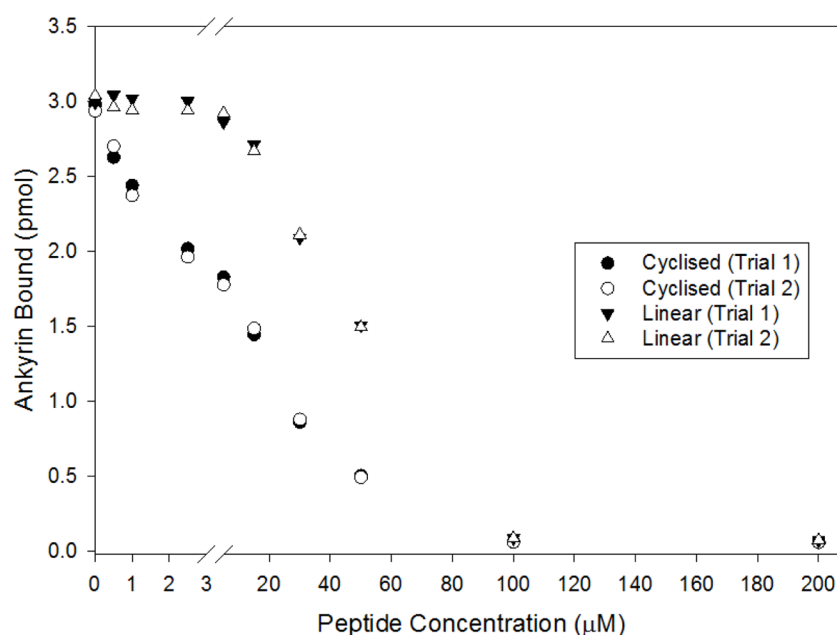


**Figure 3.**

Inhibition of D<sub>3</sub>D<sub>4</sub> ankyrin binding to cdB3 by increasing concentrations of the peptide comprising residues 63–73 (loop 1) of cdB3. A loop 1 mimetic peptide was synthesized from residues 63–73 of cdB3 by modifying the peptide to contain a cysteine residue at each end. A cyclic form of the peptide was formed by air oxidation followed by C<sub>18</sub> reverse phase HPLC, while the linearized form was obtained by incubating the cyclized peptide in 1 mM dithiothreitol. Both peptide compositions were confirmed by mass spectrometry. After incubation of D<sub>3</sub>D<sub>4</sub> ankyrin and cdB3 (His-tagged) in the presence of increasing concentrations of peptide, complexes were captured on Co<sup>2+</sup>-NTA beads, washed and eluted as before, and assayed for bound GST-D<sub>3</sub>D<sub>4</sub> ankyrin by analysis of GST activity. Error bars correspond to S.D., where n=2.

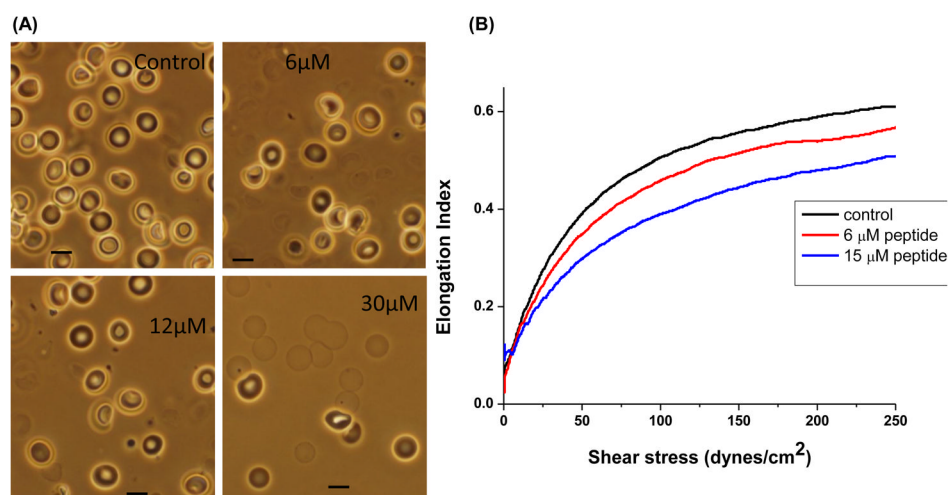


**Figure 4.**

Effect of resealing the cyclized loop 1 peptide into human erythrocytes on red cell morphology and deformability. (A) Washed fresh red cells were suspended in PBS containing 5 mM glucose, 2 mM MgCl<sub>2</sub> and the indicated concentrations of cyclized peptide. After flash freezing in liquid N<sub>2</sub> to lyse cells, cells were thawed at room temperature and resealed with entrapped peptide by incubation for 45 min at 37°C. Extracellular peptide was then removed by washing 4x with PBS containing 5 mM glucose and 0.5% bovine serum albumin, and resealed ghosts were examined with a 100x oil immersion lens by light microscopy. As peptide concentration increased, cell diameters were observed to decrease and membrane fragments became more prominent (bar = 10 microns). (B) Analysis of the effect of resealing, 6 or 15  $\mu\text{M}$  cyclic peptide on the deformability of the resealed ghosts by ektacytometry. In this method, the resealed ghosts are subjected to a gradually increasing shear stress and the ratio of their axis perpendicular to the shear force to their axis parallel to the shear force (elongation index) is taken as a measure of the ability of the membranes to deform in response to the shear force.

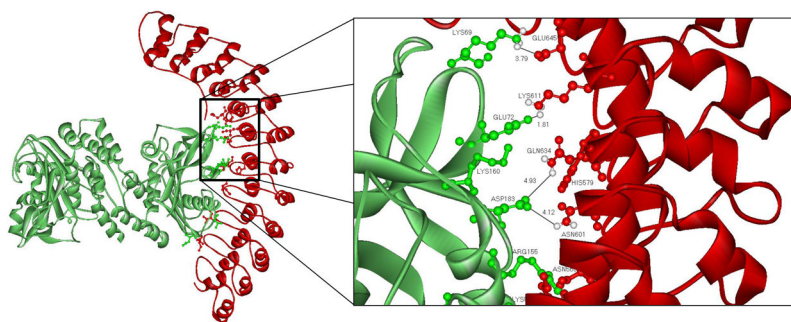


**Figure 5.**

Simulated docking of cdB3 on the D<sub>3</sub>D<sub>4</sub> domain of ankyrin. Weak interactions are predicted between the following residues: Lys 69 (cdB3)-Glu 645 (Ank); Glu 72 (cdB3)-Lys 611 (Ank); Asp 183 (cdB3)-Gln 634/Glu 645 (Ank); Lys 160 (cdB3)-His 579 (Ank); Arg 155 (cdB3)-Asn 568 (Ank); Glu 151 (cdB3)-Lys 535 (Ank); Thr 126 (cdB3)-Thr 500 (Ank); and Gln 124 (cdB3)-Asp 649 (Ank). Evaluation of this interfacial orientation is provided in the mutagenesis studies described in the text.

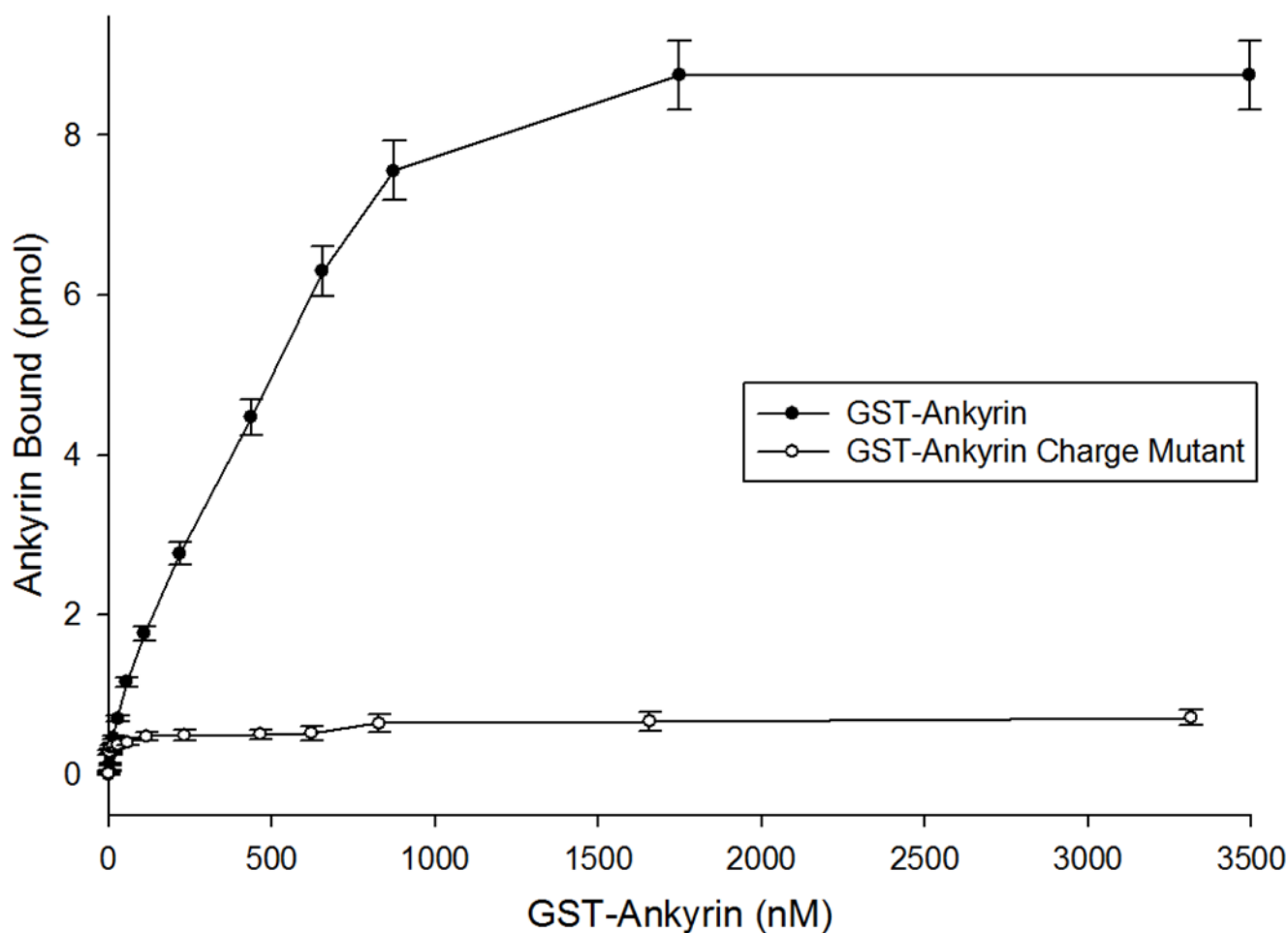


**Figure 6.**

Effect of mutating ankyrin residues predicted to participate in cdB3 binding on the affinity of GST-ankyrin for cdB3. Binding experiments were performed as previously described (see Methods). Complexes formed between His-tagged cdB3 and either native or mutated GST-D<sub>3</sub>D<sub>4</sub> ankyrin were evaluated by measuring the GST activity associated with the GST-D<sub>3</sub>D<sub>4</sub> ankyrin. Because of their prominent contributions to the predicted interfacial weak bonds shown in Fig. 5, the following mutations were examined for their effect on cdB3 affinity: N601D, K611E, Q634E, and E645K. Wild-type ankyrin was found to bind to cdB3 with an apparent dissociation constant of ~400 nM, whereas the above mutant showed no affinity for cdB3. Error bars correspond to S.D., where n=2.